Geomechanics and Engineering, *Vol. 23, No. 6 (2020) 575-585*
DOI: https://doi.org/10.12989/gae.2020.23.6.575

Basin edge effect on industrial structures damage pattern at clayey basins

Hadi Khanbabazadeh[a], Abdullah C. Zulfikar[b] and Ali Yesilyurt*

Department of Civil Engineering, Gebze Technical University, 41400 Gebze, Kocaeli, Turkey

(Received September 22, 2020, Revised December 5, 2020, Accepted December 17, 2020)

Abstract. In this numerical study, the 2D dynamic behavior of a clayey basin and its effect on damage pattern over basin edge are investigated. To attain this goal, a fully nonlinear time domain analysis method has been applied. Then, the fragility curves of the considered two typical industrial structures for that certain point are estimated using the acceleration time histories recorded at each surface point. The results show that the use of the damage related parameters in site effect analyses, instead of amplification curves, can yield more realistic estimation of the basin dynamic response. In a distance about 150 m from outcrop at the basin edge, the differences between fragility curves increase when increasing the distance from outcrop with respect to the reference rock site. Outside this region and towards the basin center, they tend to occur in rather single curves. Furthermore, to connect the structural damage to the basin edge effect, the earthquake demand value at different points for two typical structures was evaluated. It was seen that the probability of occurrence of damage increases over 250 m from outcrop, while the effect of the basin edge was limited to 150 m in case of the basin edge evaluation by using fragility curves.

Keywords: site effect; basin edge effect; 2D dynamic behavior; fragility curve

1. Introduction

The fact that the damage pattern of the sedimentary sites is higher with respect to the hard sites has been proved during several earthquakes. This kind of effect is known as the site effect (Assimaki and Gazetas 2004, Abraham *et al.* 2015, Gautam *et al.* 2016, Zhu *et al.* 2018, Costanzo *et al.* 2019, Mayoral *et al.* 2019). In addition to that, the existence of the inclined bedrock at the sides of the basins causes the concentration of the damage at these parts, which is known as the basin edge effect. These effects influence the specifications of the bedrock motion such as PGA, frequency content and duration (Zhu and Thambiratnam 2016, Riga *et al.* 2016, Falconea *et al.* 2018). Several studies have revealed the effect of 2D bedrock on distribution of damage (Bakir *et al.* 2002, Abraham *et al.* 2016, Khanbabazadeh *et al.* 2018).

After the pioneering semi-analytical/semi-numerical work of Aki and Larner (1970) several analytical and numerical methods have been applied in the investigation of the different aspects of the site effect (Paolucci 1999, Faccioli *et al.* 2002, Rodriguez-Castellanos *et al.* 2011, Kham *et al.* 2013). In some situations, the local site effect can be inferred reasonably by using simple 1D models. However, lateral heterogeneity at alluvial basins may give rise to focusing and locally generated surface waves (Makra and Chavez-Garci 2016, Madiai *et al.* 2016, Yniesta *et al.* 2017, Stanko *et al.* 2019). Several field and numerical investigations have shown the insufficiency of the approaches based on 1D site response (Beyen and Erdik 2004, Khanbabazadeh *et al.* 2019). To obtain better estimation of the dynamic behavior of basins with different geometries during earthquakes, the application of 2D and 3D analytical methods have gained popularity among researchers (Semblat *et al.* 2005, Makra *et al.* 2005, Manakou *et al.* 2010, Khanbabazadeh and Iyisan 2014a and b, Saenz *et al.* 2019). The finite element and finite difference methods, the boundary element method (direct and indirect methods) and hybrid techniques are among the most used analytical methods (Heymsfield 2000, Alvarez *et al.* 2004, Kamalian *et al.* 2006, Tsai and Liu 2017, Riga *et al.* 2018). Because of its flexibility in the modeling of the irregular geometries and nonlinear behavior of soil, the use of finite difference method is among the successful examples of the application of the numerical methods in 2D and 3D site effect analysis (Frankel 1993).

In practice, the dynamic behavior of the basins is generally presented by the maximum spectral amplification factor (MSAF) curves. To obtain these curves, the maximum ratio of the response spectrum at each surface point to the reference rock site is estimated (Safak 2001, Gelagoti *et al.* 2010). However, the investigation of 2D dynamic response using the MSAF curves remains somewhat misleading because these maximums do not occur at the same period (Khanbabazadeh *et al.* 2018, Iyisan and Khanbabazadeh 2013). In this study, since the selected structures are on the surface, there is no need for consideration of SSI. Nevertheless, for structures that SSI matters, it must be considered in evaluation of their damage. Besides, despite greater MSAF at certain region of basin surface, the results of the damage analyses can present less damage with

*Corresponding author, Ph.D. Student
E-mail: aliyesilyurt@gtu.edu.tr
[a]Ph.D.
E-mail: hadikhanbabazadeh@gmail.com
[b]Ph.D.
E-mail: can.zulfikar@gmail.com

Copyright © 2020 Techno-Press, Ltd.

ISSN: 2005-307X (Print), 2092-6219 (Online)

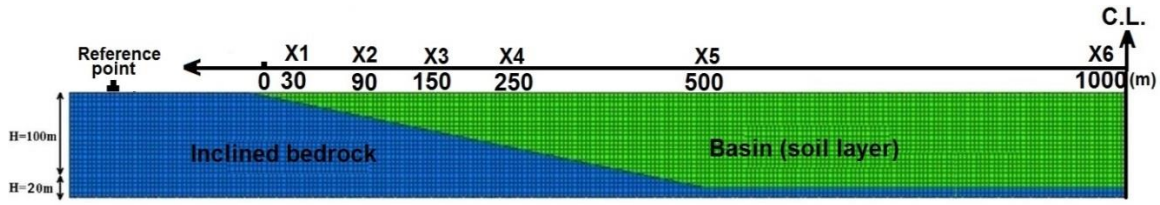

Fig. 1 The schematic geometry of the modeled basin and the reference structure at free-field

Table 1 The geotechnical properties of the selected soil material

Soil Type	c (kPa)	ϕ(°)	Vs (m/s)	G (MPa)	K (MPa)	γ (kN/m^3)
Medium Plasticity Clay	75~90	10	200~400	7.6e4~33.6e4	2e5~8.8e5	19~21
Elastic Bedrock (elastic)	-	-	1000	2500	4160	25

respect to the region with smaller MSAF. This is related to the effect of the interference and mixing of different frequency components affecting the structural damage, which is missing in the MSAF curves. Since the final purpose of the site effect studies is to see the site response and the edge effect on the buildings, this study investigates the effect of the basin edge on the damage pattern. The aim of this study is to relate the dynamic behavior of a clayey 2D basin to damage ratio (DR) of structures. Damage ratio is defined as the ratio of the earthquake damage repairing cost to the replacement cost for the structure (Askan and Yucemen 2010). To this end, a 2D clayey basin with bedrock inclination at its sides is subjected to a set of strong ground motions, and the acceleration time histories at different points of the basin surface are recorded in time domain for each bedrock motion. The dynamic analyses of the basin are done by a fully nonlinear time domain method which is based on explicit finite difference scheme. Then, the fragility curves of the two typical structures at each surface point are estimated using the recorded acceleration time histories.

The performance based analyses of the selected structures are done using the incremental dynamic analysis (IDA) using IDARC2D (Reinhorn *et al.* 2009). Then, the effect of the basin edge on variation of the damage ratio will be studied by evaluation of the damage probability matrix (DPM) and mean damage ratio (MDR) at each surface point.

2. Basin model and structural properties

The purpose of this study is to relate the dynamic behavior of a 2D clayey basin to damage ratio of structures. To this end, a hypothetical basin with a bedrock inclination of 10° at the basin edges and 100 m of depth was selected. Since the geological investigations show the greater statistical frequency of the inclinations between 5° to 15°, and because of the longer projection distance of these smaller angles at the basin surface, the effect of this inclination range draws more attention in engineering works. Thus, the bedrock inclination of 10° has been investigated in this study. In order to completely catch basin edge effect, the basin width has been taken too long (2000 m) so that these effects are caught. If the results show the influence of inclined bedrock beyond basin edge, the width can be increased. The analyses results have shown the sufficiency of the selected width to depth ratio for these set of analyses. Fig. 1 shows the schematic geometry of the basin as well as the reference point at free-field.

To make the results useful at engineering issues, the clay type has been selected with respect to the soil classification codes. This soil is classified as medium plasticity clay. A linear variation of the properties over 100 m basin depth has been provided as in Table 1. Also, the clay is assumed normally consolidated.

In this study, typical single-story reinforced concrete (RC) industrial structure, which is generally preferred in organized industrial zones, has been taken into consideration. The considered two existing typical single-story structures with different geometric dimensions and column types are presented in Fig. 2 and Table 2.

Both of the studied structures have square column cross-sections. The frames are composed of cantilever columns with rigid joints at the bottom (on foundation level). At the columns top, the pre-stressed precast beams have got pinned connections at roof levels. Thus, the lateral loads are carried out by the columns stiffness along X and Y axes directions.

To define the structural damage under earthquake effects, the bearing characteristics of the column cross sections have been given by the moment-curvature relationship (M-ϕ). This relationship is presented by a tri-linear curve with three characteristic points based on the Mander unconfined and confined concrete model. The utilized moment-curvature relationship has obtained using the software XTRACT v3.0.7 (2006). Table 2 presents the specifications of the inner and outer columns of the considered structures.

The idealized 2D model of the clayey basin is subjected to the collection of 16 strong ground motions. Several criteria have been applied in selection of the strong ground motion set. The used motion set comprises sixteen earthquakes with four peak ground acceleration (PGA) levels of 0.1 g, 0.2 g, 0.3 g and 0.4 g; four motions for each PGA level. This set includes records of different frequency

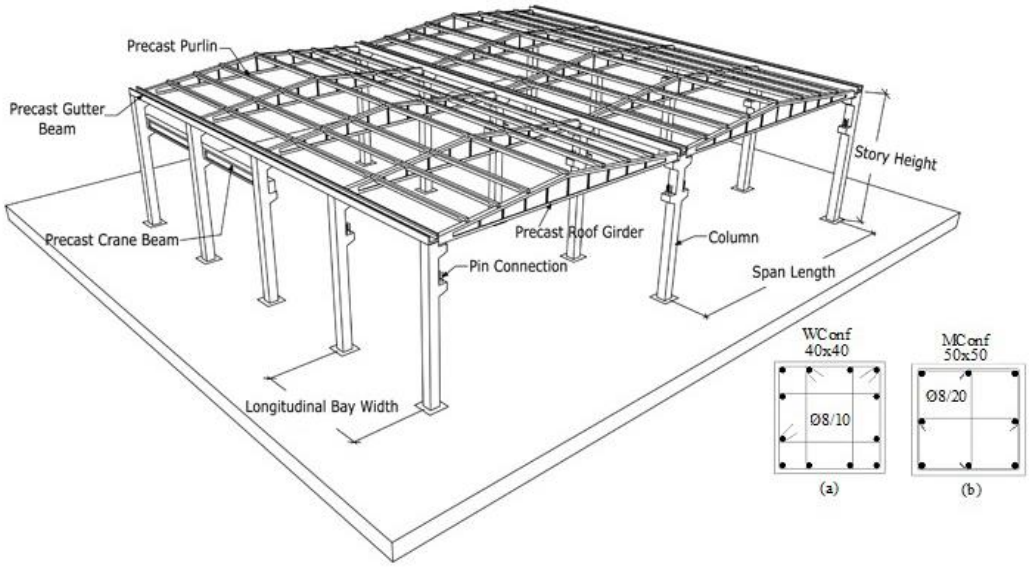

Fig. 2 The typical single-story industrial structures configuration specification (a) type I and (b) type II

Table 2 The geometrical and structural properties of the inner and outer columns of the selected structures

Column Section	Height	Span length	Bay Width	T	Column Location	EI initial	Mcr	My	Øy	Øu	EIpy
	m	m	m	sec		kN.mm^2	kN.mm	kN.mm	rad/mm	rad/mm	kN.mm^2
Type I 40x40 (ρ=%1.5&WConf	6.5	22	7.2	1.75	Outer	5.69E+10	3.98E+04	1.93E+05	1.09E-05	3.75E-04	6.21E+07
					Inner	6.14E+10	4.45E+04	2.06E+05	1.10E-05	3.64E-04	6.12E+07
Type II 50X50 (ρ=%1.5&MConf)	7.5	15	7.6	1.3	Outer	1.278E+11	6.67E+04	3.65E+05	7.64E-06	1.87E-04	2.76E+08
					Inner	1.44E+11	7.62E+04	3.77E+05	7.67E-06	1.78E-04	2.73E+08

Table 3 The specifications of the selected earthquakes

	Earthquakes	Station	Amax (g)	Magnitude	Significant Duration (s)	Arias Intensity (m/s)
1	Palm springs (1986)	Silent Valley	0.1	M_L=5.9	6.14	0.0658
2	Chalfant (1986)	LongValleyDam	0.1	Mw=6.2	10.24	0.0638
3	Mammoth lakes (1980)	LongValleyDam	0.1	Mw=6.0	7.46	0.0666
4	Anza (1980)	PinyonFlat	0.1	Mw=4.9	1.945	0.0218
5	Sakarya (1999)	Development burea	0.2	Md=5.7	3.11	0.1397
6	Dinar (1995)	Dinar station	0.2	M_L=5.0	14.95	0.8096
7	Duzce (1999)	Lamont	0.2	Mw=7.1	10.57	0.5283
8	Livermore (1980)	Morgan Terr Park	0.2	Mw=5.4	3.42	0.1877
9	Mendocino 1992	EEL River valley	0.3	M_L=6.5	4.82	0.8079
10	Coyotelake (1979)	Coyote Lake Dam	0.3	Mw=5.7	3.68	0.4003
11	Parkfield (1966)	Temblor pre	0.3	Mw=6.1	4.29	0.3615
12	Firuzabad (1994)	Firuzabad-ZRT	0.3	Mw=5.9	7.14	0.687
13	Kocaeli1(1999)	Development burea	0.4	Md=7.4	9.74	1.5843
14	Parkfield (1996)	Temblorpre	0.4	Mw=6.1	3.19	0.5537
15	Umbria-Marche (1997)	Colfiorito-Casermette	0.4	Mw=4.3	4.57	0.6902
16	South Iceland (2000)	Thjorsarbru	0.4	Mw=6.5	4.29	1.6125

contents and durations. Since the scaling affects several specifications of a motion, no scaling has been applied to these motions. Ten motions of this set (except motions no. 5, 6, 7, 12, 15 and 16) have been used from PEER ground motion database, while others have been obtained from other reliable research centers such as KOERI (Turkey) and IIEES (Iran). To remove the effect of soil layers from selected accelerograms, they have been chosen from

motions recorded on stiff soils during real earthquakes, or deconvoluted to the corresponding bedrock motion. The earthquakes no. 5 (Turkey), no.12 (Iran), no.15 (Italy) and no. 16 (Iceland) have been deconvoluted to bedrock motions. The deconvolutions have been done either using the SHAKE2000 program or the deconvoluted motions have been obtained from KOERI (Turkey) and IIEES (Iran). All motions have time step of 0.005 s except Mendocino motion (with dt=0.02 s) and Parkfield motion (with dt=0.01 s). They are baseline corrected and filtered by a 25 Hz low-pass filter. Table 3 presents the specifications of the used earthquakes.

3. Analysis method

3.1 Site effect analysis

The dynamic analyses of the basin are performed using a fully nonlinear method, which is based on explicit finite difference scheme and solves the full equations of motion using FLAC3D code. Since the application of finite difference method provides flexibility in the modeling of the irregular geometries, which carries more importance at 2D analyses, this method has been used for these analyses.

The used fully nonlinear method follows any prescribed nonlinear constitutive relation. In this method, since the strain increments (not tensors) relate to the stress tensors, plastic yielding is modeled appropriately (Cundall 2008).

Also, both shear and compressional waves are propagated together in a single simulation, and the material responds to the combined effect of both components. Using a nonlinear material law, interference and mixing of different frequency components occur naturally. In this method, first-order space and time derivatives of a variable are approximated by finite differences, assuming linear variations of the variable over finite space and time intervals, respectively. Then, the continuous medium is replaced by a discrete equivalent one in which all forces involved (applied and interactive) are concentrated at the nodes of a three-dimensional mesh used in the medium representation. The application of the boundary conditions and damping are presented in the following sections.

3.1.1 Boundary conditions

The approach used in the continuum finite difference code NESSI (Cundall *et al.* 1980) is developed for FLAC3D via Free-Field boundary condition which involves the execution of free-field calculations in parallel with the main-grid analysis. It provides non-reflecting property for the vertical boundaries. For model bottom, in order to prevent the reflection of outward propagating waves back into the model, and to allow the necessary energy radiation, the quiet boundary scheme proposed by Lysmer and Kuhlemeyer (1969), which involves dashpots, are attached independently in the normal and shear directions. The schematic coupling of the main grid to free-field grids by viscous dashpots is presented at Fig. 3. Also, to prevent the numerical distortion, with respect to the frequency content of the input waves and the wave speed characteristics of the system, based on Kuhlemeyer and Lysmer (1973) the

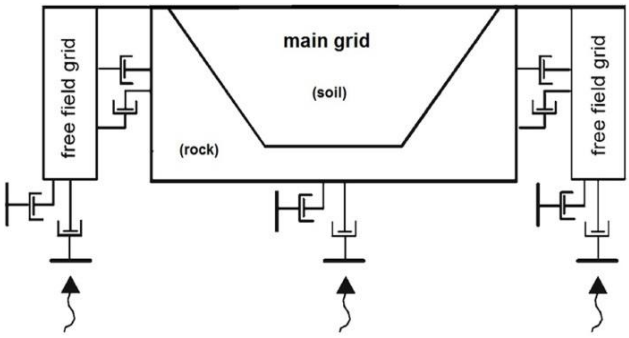

Fig. 3 The schematic coupling of the main grid to free-field grids by viscous dashpots

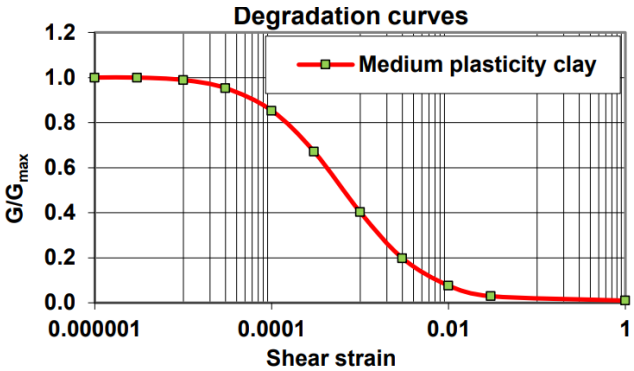

Fig. 4 The utilized degradation curves for selected soil type

spatial element size was selected smaller than one tenth to one eighth of the wavelength associated with the highest frequency component of the wave.

3.1.2 Damping

In this study, the formulation of the hysteresis damping is applied. In this case, the combination of the Hardin/Drnevich hysteretic damping with Mohr-Coulomb model is utilized. Using the hysteretic-type damping model and with no extra damping, the damping and tangent modulus are appropriate to the level of excitation at each point in time and space, since these parameters are embodied in the constitutive model. In effect, no damping curve is defined in fully nonlinear analysis. The degradation curve of the used clayey material has been obtained from Ishibashi and Zhang's (1993) work. Then, this curve was fitted to one of the FLAC's built in sigmoidal models (continuous functions) by fishes so that analytical derivatives are calculated. The utilized degradation curve for selected soil type is shown in Fig. 4. The verification of this modeling has been done by comparing to the solution of the valley studied by Kawase and Aki (1989), and presented at Iyisan and Khanbabazadeh (2013) and Khanbabazadeh *et al.* (2018).

3.2 Structural damage analysis

The incremental dynamic analysis (IDA) procedure has been applied to estimate all of the possible damage states that the structure could experience under seismic excitation conditions (Vamvatsikos and Cornell 2002). This

parametric analysis involves subjecting a structural model to a set of strong ground motions. The fundamental periods of the studied structures are considered based on the cracked section stiffness properties of the columns. Each of their spectral acceleration value (Sa) corresponding to the period of structure was scaled with 0.05 g increments in the 0.05 g-1.5 g range. The nonlinear dynamic analysis was performed using IDARC2D (Inelastic Damage Analysis of Structures) (Reinhorn *et al.* 2009). This choice was made because of its advantage for definition of several different parameters of damage due to dynamic loads (Dumova-Jovanoska 2000).

In this method, the solution of incremental system is carried out using the Newmark-Beta algorithm which uses constant average acceleration. Also, it includes a spread plasticity formulation based on the flexibility method to capture the variation of the section flexibility, and then combines them to determine the element stiffness matrix. In the non-linear dynamic analysis, the spread plasticity approach with linear flexibility distribution is used. As the structural damping, the Rayleigh damping with the coefficient of 5% is used. In this analysis, despite the small axial column loads, the P-Delta effect has been taken into consideration because of the presence of high-rise column elements (Eren and Lus 2015). The hysteretic behavior has been specified at both ends of each member by three parameters. The trilinear hysteretic model, which is energy based strength degradation hysteretic behavior, was adopted for structure to consider the effect of stiffness degradation, strength degradation and pinching (Sivaselvan and Reinhorn 2000).

3.2.1 Definition of the damage criteria

Among various parameters for assessment of damage condition such as inter-story drift ratio (Kircher *et al.* 1997, Kircil and Polat 2006) and strain base limit of the concrete and longitudinal reinforcement (Senel and Kayhan 2010, Palanci *et al.* 2017), the Park and Ang damage index (Park *et al.* 1987, Singhal and Kiremidjian 1996) is used in this study. In this model, the damage is defined as a linear combination of maximum deformations and absorbed hysteretic energy. The participation of both extreme deformations and the dissipated hysteretic energy at a lower level of deformations are among main advantages of this model. The modification of the Park and Ang damage model presented by Kunnath *et al.* (1992) is as follows:

$$DI = \frac{\theta_m - \theta_r}{\theta_u - \theta_r} + \frac{\beta}{\theta_u * M_y} * E_h \quad (1)$$

where θ_m is the maximum rotation attained during the non-linear dynamic analysis; θ_u is the ultimate rotation capacity of the section; θ_r is the recoverable rotation when unloading; M_y is the yield moment; β is a model constant parameter; and E_h is the cumulative dissipated energy in the section. The Park *et al.* (1987) damage model has been calibrated using a database of observed structural damage of reinforced concrete buildings. Table 4 presents the used calibrated damage index with the degree of observed damage in the structures.

Also, the performance assessment of the structures was fulfilled by the determination of the seismic performance of structures for a given seismic hazard levels. The mathematical description of the exceedance probability is stated as follows:

Table 4 Damage state related indexes threshold values (Park *et al.* 1987)

Damage state	Damage index
None	<0.10
Slight	0.10-0.25
Moderate	0.25-0.40
Extensive	0.40-1.0
Collapse	>1.0

$$P_{i,j} = P(DI \geq DS_i | S_{ae,j}) \quad (2)$$

where $P_{i,j}$ is the probability of structural damage index exceeding the damage state i conditioned at $S_{ae,j}$. The probabilistic distribution of the structural damage is derived by assuming a two-parameter lognormal distribution function. The probability of exceeding of a damage state (DS_i) for damage index (DI) for a given spectral acceleration (S_{ae}) is modeled as:

$$P[DS_i | S_{ae}] = \Phi\left[\frac{1}{\beta_{DS_i}} \ln\left(\frac{S_{ae}}{\overline{S}_{ae,DS_i}}\right)\right] \quad (3)$$

where $\overline{S}_{ae,DS_i}$ is the median value of spectral acceleratian at which the structure reaches the threshold of the damage state (DS_i); β_{DS_i} is the standard deviation of the spectral acceleration for i damage state; and Φ is the standard normal cumulative distribution function.

4. Results and discussion

4.1 Fragility curves

In this section, the estimated fragility curves of two different single-story RC industrial structures are presented for different basin surface points from X1 to X6 (Fig. 1) as well as reference point (free-field). Fig. 5 presents the fragility curves of the structure type I at each surface point.

In this figure, the difference between fragility curves for each damage state with respect to the reference point on rock site (free-field) can be seen. The results show the effect of the basin edge on the fragility curve. It is seen that, for all damage states, by the increase in the distance from outcrop until point X3, the difference between fragility curves at surface point with respect to the reference site increases. From this point on, the difference decreases so that at point X6 they tend to rather single curves for all damage states. Almost the same trend but with a higher difference level can be seen for the structure type II (Fig. 6). Also, almost for all damage states at points X5, the curves of the structure type II remains below the damage states of the reference rock site.

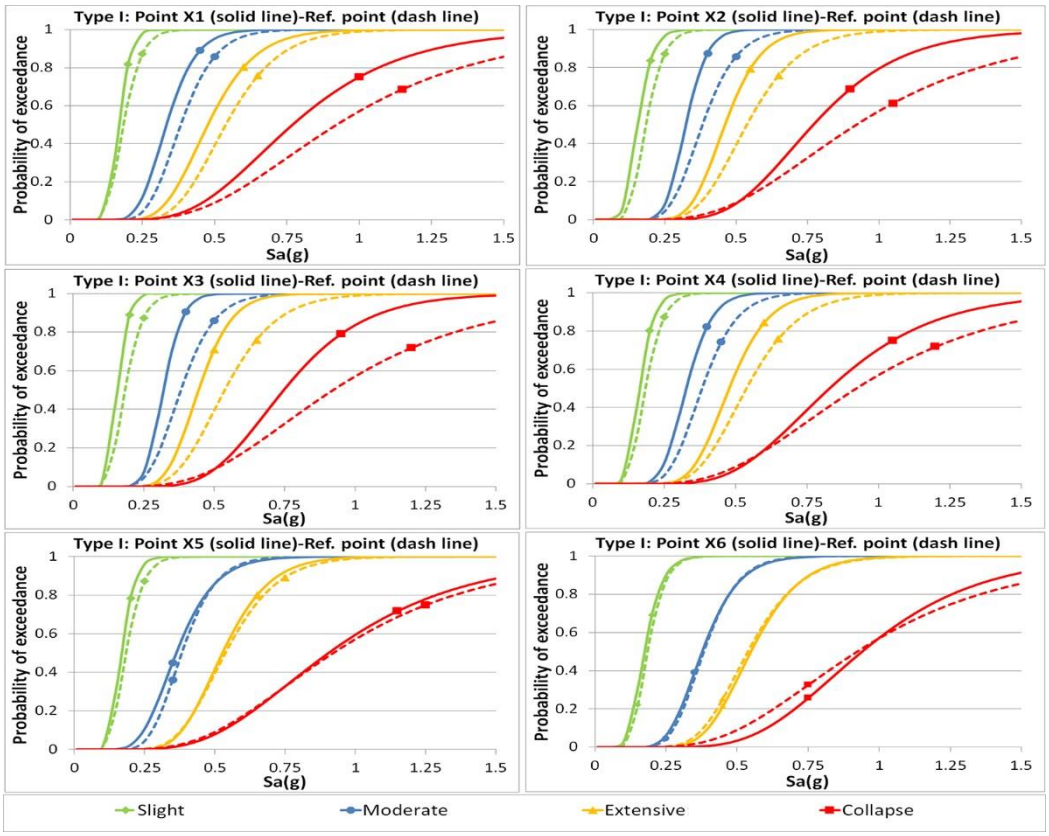

Fig. 5 The fragility curves of the structure type I in different surface point

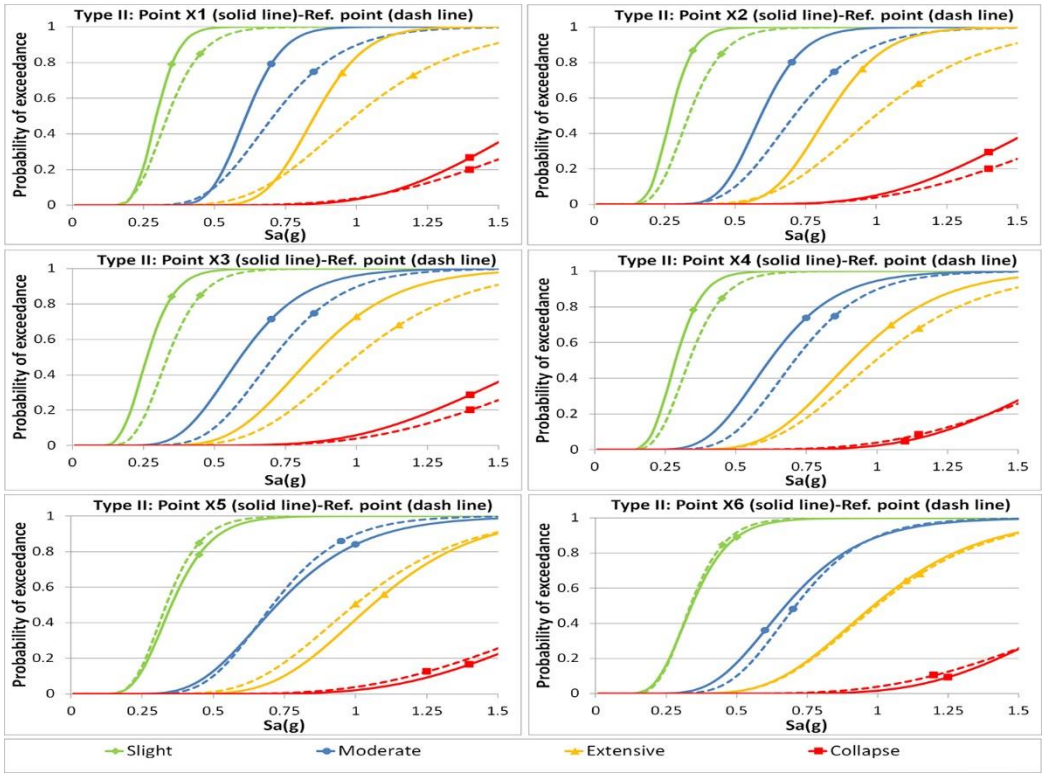

Fig. 6 The fragility curves of the structure type II in different surface point

4.2 Damage probability matrix

Figs. 5 and 6 present just the change in fragility curve under the effect of the basin edge. In order to study the variation of structural damage over the basin surface, the earthquake demand value at different points should be

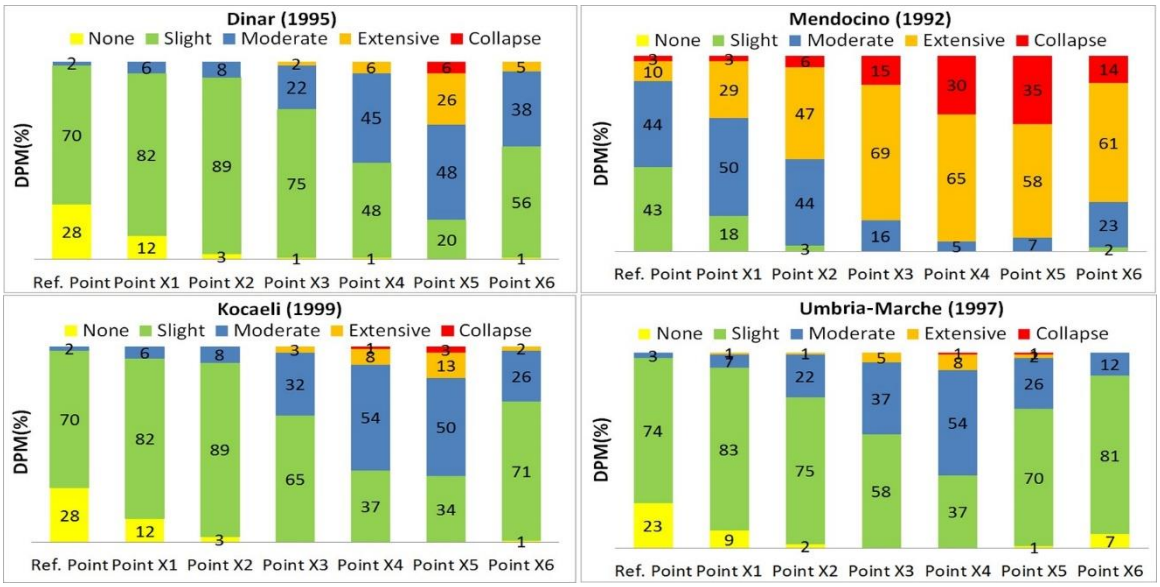

Fig. 7 The DPMs of the structure type I under the effect of selected four earthquakes

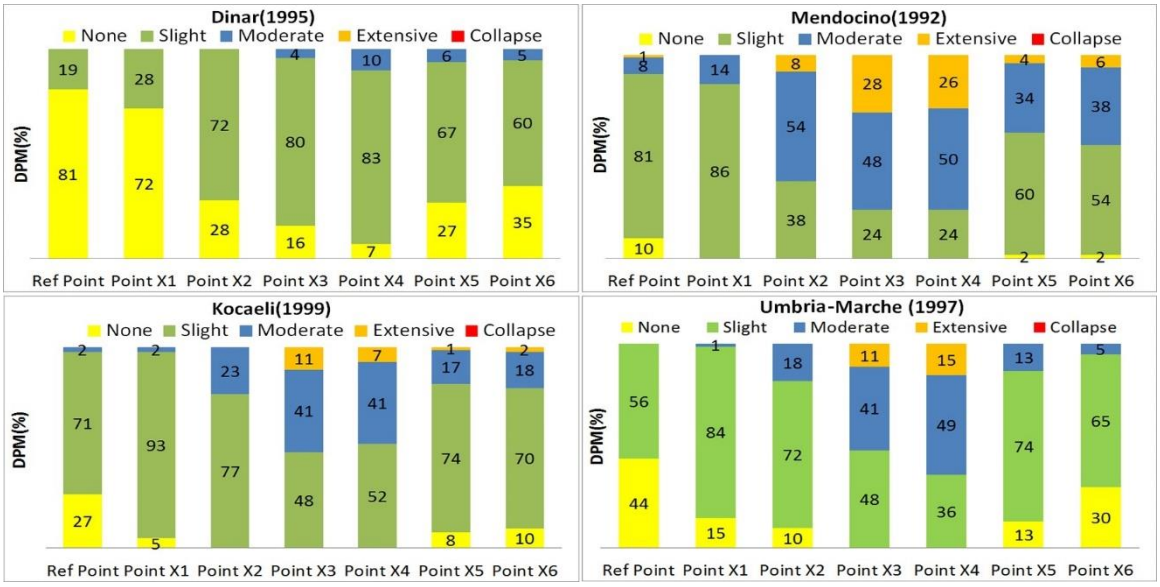

Fig. 8 The DPMs of the structure type II under the effect of selected four earthquakes

considered. To this end, the damage probability matrix (DPM) was evaluated for considered two structures with respect to their locations at the basin surface. A damage state in a DPM is defined as the degree of damage to a given typical building under an earthquake of a specific intensity. Each value in a DPM represents the probability of occurrence of the specific level of damage for a given structure, under an absolute spectral acceleration of ground motion. Using the incremental dynamic analysis, $P(DS_i|S_{ae,j})$ values can be calculated from:

$$P(DS_i|S_{ae,j}) = \frac{N[P(DI \geq DS_i|S_{ae,j})]}{TE} \quad (4)$$

where TE is the number of the earthquake in the IDA subjected to structure and $N[P(DI \geq DS_i|S_{ae,j})]$ is the number of DI, which reaches or exceeds the DS_i, among the TE. The DPM was evaluated for both considered structures under four different earthquakes from our strong ground motion set (Dinar (1995), Mendocino (1992), Kocaeli (1999) and Umbria-Marche (1997) from Table 3). Fig. 7 presents the DPMs of the structure type I under the effect of selected four earthquakes.

This figure shows the effect of the basin edge on the structural damage over basin surface. It is seen that, for example, under the effect of Kocaeli earthquake (1999) (Md=7.4, PGA=0.4 g), while the probability of occurrence of slight and moderate damages for structure type I at reference points (free-field) are 70% and 2%, respectively, the probability of occurrence of moderate damage increases to about 50% at points X4 and X5 for the same structure. In the meantime, the probability of occurrence of the extensive damage increases from 3% to 13% at points X4 and X5, respectively. Although the probability of occurrence of the collapse damage state decreases at point X6 with respect to

Table 5 CDR values proposed in different studies

Damage state (DS)	Central damage ratio (CDR) (%)	
	Gurpinar *et al.* (1978)	Askan and Yucemen (2010)
None	0	0
Slight	5	5
Moderate	30	30
Extensive	70	85
Collapse	100	85

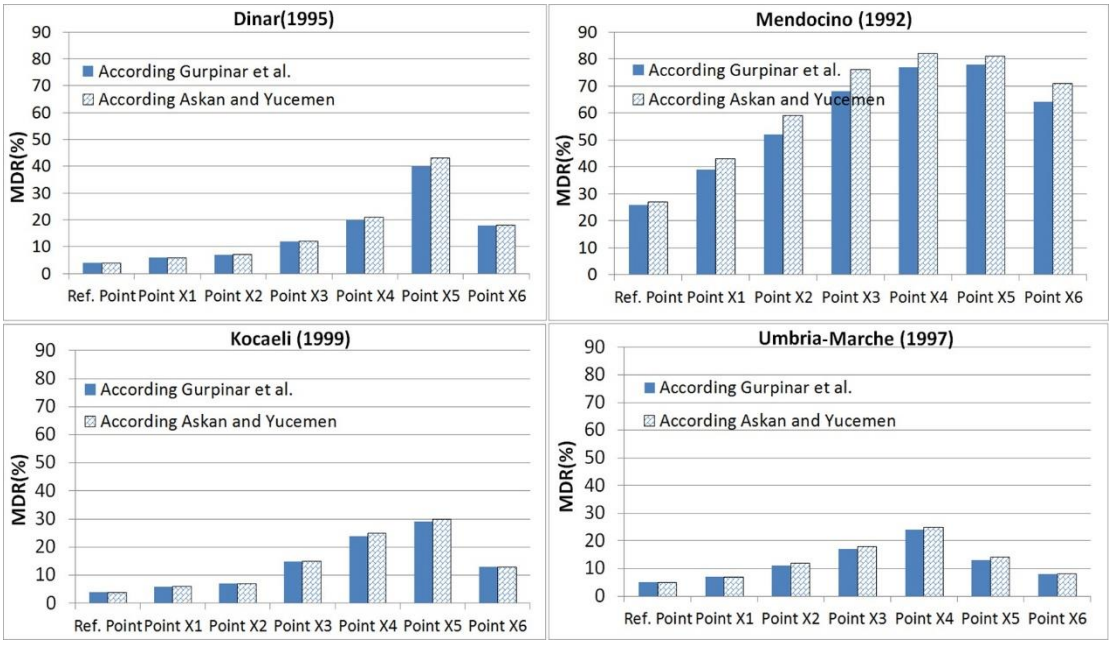

Fig. 9 The variation of MDR for structure type I under the effect of selected four motions over basin surface

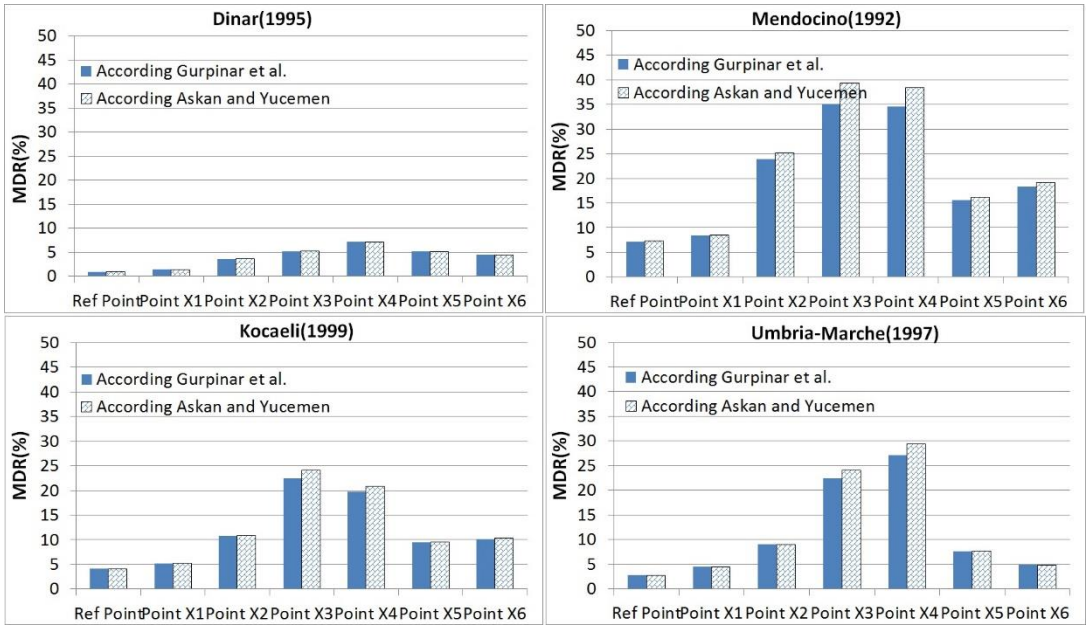

Fig. 10 The variation of MDR for structure type II under the effect of selected four motions over basin surface

point X5, the probability of occurrence of the moderate damage is higher with respect to the reference rock site. As another example, the DPM of the structure type I under the effect of the Mendocino earthquake (1992) (ML=6.5, PGA=0.3 g) can be dealt with. The results show that while the probability of occurrence of the collapse damage state

for structure type I is about 3% at the free-field, because of the basin edge effect, it increases to 35% at point X5, and decreases to 14% at point X6. Also, in Fig. 8 the DPMs of the structure type II under the effect of selected four earthquakes is presented. It is seen that the variation of the damage pattern under the effect of the basin edge changes by the change in structure specification.

4.3 Mean damage ratio

Damage ratio (DR) is defined as the ratio of the earthquake damage repairing cost to the replacement cost for the structure. Expressing damage with a single value rather than to express the probability of damage of four different damage situations is called the mean damage ratio (MDR), which is defined as follows:

$$\mathrm{MDR}\left(\mathrm{S_{ae,j}}\right) = \sum_{\mathrm{DS}} \mathrm{P}\left(\mathrm{DS_i}|\mathrm{S_{ae,j}}\right) * \mathrm{CDR}(\mathrm{DS_i}) \qquad (5)$$

where $\mathrm{MDR}\left(\mathrm{S_{ae,j}}\right)$ is the mean damage ratio corresponding to the intensity level $\mathrm{S_{ae,j}}$; and $\mathrm{CDR(DS)}$ is the central damage ratio corresponding to damage state $\mathrm{DS_i}$. In obtaining MDR values, the seismicity of the region, the characteristics of the structure and the CDR values are important. In this study, the MDR values for the considered structures at 7 different points (including reference point) were evaluated. Table 5 presents CDR values for four different damage states proposed by Gurpinar *et al.* (1978) and Askan and Yucemen (2010).

Fig. 9 presents the variation of MDR for structure type I under the effect of selected four motions over basin surface using CDR values. This figure clearly presents the effect of the basin edge on the damage ratio of a typical single-story RC industrial structure over the studied clayey basin. It is seen that for the studied 2D alluvial basin and for all applied earthquake motions, the MDR increases as the distance from outcrop increases.

It generally reaches to highest values at points X4 and X5, and then decreases at point X6. The location of point X6 has been selected in a distance which is far enough from the outcrop that is not affected by the inclined bedrock. Thus, the damage ratio at point X6 represents the 1D behavior of the basin at central parts. Moreover, it is seen that Mendocino earthquake (1992) with PGA of 0.3 g causes more damage ratio at basin edge when it is compared to Kocaeli (1999) and to Umbria-Marche (1997) earthquakes with higher PGA (0.4 g). Furthermore, the variation of MDR for structure type II has been presented in Fig. 10. Compared to structure type I, it is seen that although the variation of the MDR under the effect of the basin edge has similar trend, its damage level changes by the change in structure specification.

5. Conclusions

As it was mentioned earlier, the final purpose of the site response and basin edge effect studies is to determine its effect on the buildings performance. Since the basin edge affects the frequency content of the motion throughout basin surface, and the MSAFs don't occur at the same period, the investigation of 2D dynamic response using this parameter remains somewhat misleading. For these reasons, the greater MSAF doesn't necessarily result in higher damage in the buildings. In this study, the effect of the basin edge on the damage ratio was studied. In this study, the damage ratio of two typical one story structures located on the same soil type (clay) but at different distances from bedrock outcrop was estimated. To this end, using a fully nonlinear time domain analysis method, the acceleration time histories of a set of bedrock motions were recorded at different points of the 2D basin surface. Then, using the acceleration time histories recorded at each surface point, the fragility curve of the considered structures for that certain point was estimated.

The results show that, in certain region at the basin edge, by the increase in the distance from outcrop, the difference between fragility curves at surface point with respect to the reference site increases. Although the difference level is affected by the type of structures, the length of this region is about 150 m from outcrop in case of 10◦ bedrock inclination. Outside this region, the difference decreases so that towards the basin center they tend to a rather single curves at about 500 m from outcrop.

Although the estimated fragility curves at each surface point include the effect of the basin edge, they provide no information about the variation of structural damage. To connect the structural damage to the basin edge effect, the earthquake demand value at different points for two typical structures was evaluated. The results showed that inside a certain region, the probability of occurrence of damage levels increases by the increase of distance from outcrop. The probability of occurrence of damage increases over 250 m from outcrop, while the effect of the basin edge was limited to 150 m in case of the basin edge evaluation by using fragility curves. Almost the same pattern but with different intensity level can be seen by changing the structure type. Finally, for simplicity, the damage ratio is used to express the probability of damage with a single value. It was seen that the region with critical damage ratio is in between 250 m and 500 m from the outcrop.

Based on the results of this study, it is concluded that the evaluation of site effect by connecting it to damage level, instead of the amplification curves, can yield more realistic results. It worths mentioning that damage level cannot be solely related to basin response and site effect. Since by the use of damage related parameters the effects of the frequency content are considered in more effective way, therefore, in addition to the amplification coefficients the damage parameters can be considered in seismic codes as well.

References

Abraham, J.R., Lai, C.G. and Papageorgiou, A. (2015), "Basin-effects observed during the 2012 Emilia earthquake sequence in Northern Italy", *Soil Dyn. Earthq. Eng.*, **78**, 230-242. https://doi.org/10.1016/j.soildyn.2015.08.007.

Abraham, J.R., Smerzini, C., Paolucci, R. and Lai, C.G. (2016), "Numerical study on basin-edge effects in the seismic response

of the Gubbio valley, Central Italy", *B. Earthq. Eng.*, **14**(6), 1437-1459. https://doi.org/10.1007/s10518-016-9890-y.

Alvarez, S., Sanchez-Sesma, F.J., Benito, J. and Alarcon, E. (2004), "The direct boundary element method: 2D site effects assessment on laterally varying layered media (methodology)", *Soil Dyn. Earthq. Eng.*, **24**(2), 167-180. https://doi.org/10.1016/j.soildyn.2003.09.003.

Askan, A. and Yucemen, M.S. (2010), "Probabilistic methods for the estimation of potential seismic damage: Application to reinforced concrete buildings in Turkey", *Struct. Saf.*, **32**(4), 262-271. https://doi.org/10.1016/j.strusafe.2010.04.001.

Assimaki, D. and Gazetas, G. (2004), "Soil and topographic amplification on canyon banks and the 1999 Athens earthquake", *J. Earthq. Eng.*, **8**(1), 1-43. https://doi.org/10.1142/S1363246904001250.

Bakir, B.S., Ozkan, M.Y. and Ciliz, S. (2002), "Effects of basin edge on the distribution of damage in 1995 Dinar, Turkey earthquake", *Soil Dyn. Earthq. Eng.*, **22**(4), 335-345. https://doi.org/10.1016/S0267-7261(02)00015-5.

Beyen, K. and Erdik, M. (2004), "Two-dimensional nonlinear site response analysis of Adapazarı plain and predictions inferred from aftersh ocks of the Kocaeli earthquake of 17 August 1999", *Soil Dyn. Earthq. Eng.*, **24**(3), 261-279. https://doi.org/10.1016/j.soildyn.2003.10.009.

Costanzo, A., d'Onofrio, A. and Silvestri, F. (2019), "Seismic response of a geological, historical and architectural site: The Gerace cliff (southern Italy)", *B. Eng. Geol. Environ.*, **78**(8), 5617-5633. https://doi.org/10.1007/s10064-019-01515-0.

Cundall P.A. (2008), *FLAC3D Manual: A computer program for fast Lagrangian analysis of Continua (Version 4.0)*, Minneapolis, Minnesota, U.S.A

Cundall, P.A., Hansteen, H., Lacasse, S. and Selnes, P.B. (1980), "NESSI—soil structure interaction program for dynamic and static problems", Report 51508-9, Norwegian Geotechnical Institute.

Dumova-Jovanoska, E. (2000), "Fragility curves for reinforced concrete structures in Skopje (Macedonia) region", *Soil Dyn. Earth. Eng.*, **19**(6), 455-466. https://doi.org/10.1016/S0267-7261(00)00017-8.

Eren, C. and Lus, H. (2015), "A risk based PML estimation method for single-storey reinforced concrete industrial buildings and its impact on earthquake insurance rates", *B. Earthq. Eng.*, **13**(7), 2169-2195. https://doi.org/10.1007/s10518-014-9712-z.

Faccioli, E., Vanini, M. and Frassine, L. (2002), "Complex site effects in earthquake ground motion, including topography", *Proceedings of the 12th European Conference on Earthquake Engineering*, London, U.K., September.

Falconea, G., Boldinib, D. and Amorosi, A. (2018), "Site response analysis of an urban area: A multi-dimensional and non-linear approach", *Soil Dyn. Earthq. Eng.*, **109**, 33-45. https://doi.org/10.1016/j.soildyn.2018.02.026.

Frankel, A. (1993), "Three dimensional simulation of ground motion in the Santa Bernardino Valley, California, for hypothetical earthquake on the San Andreas fault", *B. Seismol. Soc. Am.*, **83**(4), 1020-1041.

Gautam, D., Forte, G. and Rodrigues, H. (2016), "Site effects and associated structural damage analysis in Kathmandu Valley, Nepal", *Earthq. Struct.*, **10**(5), 1013-1032. https://doi.org/10.12989/eas.2016.10.5.1013.

Gelagoti, F., Kourkoulis, R., Anastasopoulos, I., Tazoh, T. and Gazetas, G. (2010), "Seismic wave propagation in a very soft alluvial valley: Sensitivity to ground-motion details and soil nonlinearity, and generation of a parasitic vertical component", *B. Seismol. Soc. Am.*, **100**(6), 3035-3054. https://doi.org/10.1785/0120100002.

Gurpinar, A., Abalı, M., Yucemen, M.S. and Yesilcay, Y. (1978), "Feasibility of mandatory earthquake insurance in Turkey", Earthquake Engineering Research Center, Report No. 78-05, Middle East Technical University, Ankara, Turkey (in Turkish).

Heymsfield, E. (2000), "Two-dimensional scattering of SH waves in a soil layer underlain with bedrock", *Soil Dyn. Earthq. Eng.*, **19**(7), 489-500. https://doi.org/10.1016/S0267-7261(00)00030-0.

Ishibashi, I. and Zhang, X. (1993), "Unified dynamic shear moduli and damping ratios of sand and clay", *Soils Found.*, **33**(1), 182-191. https://doi.org/10.3208/sandf1972.33.182.

Iyisan, R. and Khanbabazadeh, H. (2013), "A numerical study on the basin edge effect on soil amplification", *B. Earthq. Eng.*, **11**(5), 1305-1323. https://doi.org/10.1007/s10518-013-9451-6.

Kamalian, M., Jafari, M.K., Sohrabi-Bidar, A., Razmkhah, A. and Gatmiri, B. (2006), "Time domain two-dimensional site response analysis of non-homogeneous topographic structures by a hybrid BE/FE method", *Soil Dyn. Earthq. Eng.*, **26**, 753-765. https://doi.org/10.1016/j.soildyn.2005.12.008.

Kawase, H. and Aki, K. (1989), "A study on the response of a soft basin for incident. S, P and Rayleigh waves with special reference to the long duration observed in Mexico City", *B. Seismol. Soc. Am.*, **79**(5), 1361-1382.

Khanbabazadeh, H. and Iyisan, R. (2014a), "A numerical study on the 2D behavior of clayey basins", *Soil Dyn. Earthq. Eng.*, **66**, 31-41. https://doi.org/10.1016/j.soildyn.2014.06.029.

Khanbabazadeh, H. and Iyisan, R. (2014b), "A numerical study on the 2D behavior of the single and layered clayey basins", *B. Earthq. Eng.*, **12**(4), 1515-1536. https://doi.org/10.1007/s10518-014-9590-4.

Khanbabazadeh, H., Hasal, M.E. and Iyisan, R. (2019), "2D seismic response of the Duzce Basin, Turkey", *Soil Dyn. Earthq. Eng.*, **125**, 105754. https://doi.org/10.1016/j.soildyn.2019.105754.

Khanbabazadeh, H., Iyisan, R., Ansal, A. and Zulfikar, C. (2018), "Nonlinear dynamic behavior of the basins with 2D bedrock", *Soil Dyn. Earthq. Eng.*, **107**, 108-115. https://doi.org/10.1016/j.soildyn.2018.01.011.

Kircher, C.A., Nassar, A.A., Kustu, O. and Holmes, W.T. (1997), "Development of building damage functions for earthquake loss estimation", *Earthq. Spectra*, **13**(4), 663-680. https://doi.org/10.1193/1.1585974.

Kircil, M.S. and Polat, Z. (2006), "Fragility analysis of mid-rise R/C frame buildings", *Eng. Struct.*, **28**(9), 1335-1345. https://doi.org/10.1016/j.engstruct.2006.01.004.

Kuhlemeyer, R.L. and Lysmer, J. (1973), "Finite element method accuracy for wave propagation problems", *J. Soil Mech. Found. Div.*, **99**, 421-427.

Kunnath, S.K., Reinhorn, A.M. and Lobo, R.F. (1992b), "IDARC version 3.0: A program for the inelastic damage analysis of Reinforced Concrete structures", Report No. NCEER-92-0022, National Center for Earthquake Engineering Research, University at Buffalo, The State University of New York, New York, U.S.A.

Lysmer, J. and Kuhlemeyer, R.L. (1969), "Finite dynamic model for infinite media", *J. Eng. Mech. Div.*, **95**(4), 859-878.

Madiai, C., Facciorusso, J., Gargini, E. and Baglione, M. (2016), "1D versus 2D site effects from numerical analyses on a cross section at Barberino di Mugello (Tuscany, Italy)", *Procedia Eng.*, **158**, 499-504. https://doi.org/10.1016/j.proeng.2016.08.479.

Makra, K. and Chavez-Garci, F.J. (2016), "Site effects in 3D basins using 1D and 2D models: an evaluation of the differences based on simulations of the seismic response of Euroseistest", *B. Earthq. Eng.*, **14**(4), 1177-1194. https://doi.org/10.1007/s10518-015-9862-7.

Makra, K., Chavez-Garcia, F.J., Raptakis, D. and Pitilakis, K. (2005), "Parametric analysis of the seismic response of a 2D sedimentary valley: Implications for code implementations of

complex site effects", *Soil Dyn. Earthq. Eng.*, **25**, 303-315. https://doi.org/10.1016/j.soildyn.2005.02.003.

Manakou, M.V., Raptakis, D.G., Chavez-Garci, F.J., Apostolidis, P.I. and Pitilakis, K.D. (2010), "3D soil structure of the Mygdonian basin for site response analysis", *Soil Dyn. Earthq. Eng.*, **30**(11), 1198-1211. https://doi.org/10.1016/j.soildyn.2010.04.027.

Mayoral, J.M., Asimaki, D., Tepalcapa, S., Wood, C., Sancha, A.R., Hutchinson, T., Franke, K. and Montalva, G. (2019), "Site effects in Mexico City basin: Past and present", *Soil Dyn. Earthq. Eng.*, **121**, 369-382. https://doi.org/10.1016/j.soildyn.2019.02.028.

Palanci, M., Senel, S.M. and Kalkan, A. (2017), "Assessment of one story existing precast industrial buildings in Turkey based on fragility curves", *B. Earthq. Eng.*, **15**(1), 271-289. https://doi.org/10.1007/s10518-016-9956-x.

Paolucci, R. (1999), "Shear resonance frequencies of alluvial valleys by Rayleigh's method", *Earthq. Spectra*, **15**(3), 503-521. https://doi.org/10.1193/1.1586055.

Park, Y.J., Reinhorn, A.M. and Kunnath, S. (1987), I"DARC: Inelastic damage analysis of reinforced concrete frame-shear-wall structures", Technical Report NCEER-87-0008, State University of New York, Buffalo, New York, U.S.A.

Reinhorn, A.M., Roh, H., Sivaselvan, M., Kunnath, S.K., Valles, R.E., Madan, A. and Park, Y.J. (2009), IDARC2D Version 7.0: A Program for the Inelastic Damage Analysis of Structures (MCEER-09-0006).

Riga, E., Makra, K. and Pitilakis, K. (2016), "Aggravation factors for seismic response of sedimentary basins: A code oriented parametric study", *Soil Dyn. Earthq. Eng.*, **91**, 116-132. https://doi.org/10.1016/j.soildyn.2016.09.048.

Riga, E., Makra, K. and Pitilakis, K. (2018), "Investigation of the effects of sediments inhomogeneity and nonlinearity on aggravation factors for sedimentary basins", *Soil Dyn. Earthq. Eng.*, **110**, 284-299. https://doi.org/10.1016/j.soildyn.2018.01.016.

Saenz, M., Sierra, C., Vergara, J., Jaramillo, J. and Gomez, J. (2019), "Site specific analysis using topography conditioned response spectra", *Soil Dyn. Earthq. Eng.*, **123**, 470-497. https://doi.org/10.1016/j.soildyn.2019.03.004.

Safak, E. (2001), "Local site effects and dynamic soil behavior", *Soil Dyn. Earthq. Eng.*, **21**, 453-458. https://doi.org/10.1016/S0267-7261(01)00021-5.

Semblat, J.F., Kham, M., Parara, E., Bard, P.Y., Pitilakis, K., Makra, K. and Raptakis, D. (2005), "Seismic wave amplification: Basin geometry vs soil layering", *Soil Dyn. Earthq. Eng.*, **25**, 529-538. https://doi.org/10.1016/j.soildyn.2004.11.003.

Senel, S.M. and Kayhan, A.H. (2010), "Fragility based damage assesment in existing precast industrial buildings: A case study for Turkey", *Struct. Eng. Mech.*, **11**(1), 39-60. http://doi.org/10.12989/sem.2010.34.1.039.

Singhal, A. and Kiremidjian, A.S. (1996), "Method for probabilistic evaluation of seismic structural damage", *J. Struct. Eng.*, **122**(12), 1459-1467. https://doi.org/10.1061/(ASCE)0733-9445(1996)122:12(1459).

Sivaselvan, M.V. and Reinhorn, A.M. (2000), "Hysteretic models for deteriorating inelastic structures", *J. Eng. Mech.*, **126**(6), 633-640. https://doi.org/10.1061/(ASCE)0733-9399(2000)126:6(633).

Stanko, D., Gulerce, Z., Markusic, S. and Salic, R. (2019), "Evaluation of the site amplification factors estimated by equivalent linear site response analysis using time series and random vibration theory based approaches", *Soil Dyn. Earthq. Eng.*, **117**, 16-29. https://doi.org/10.1016/j.soildyn.2018.11.007.

Tsai, C.C. and Liu, H.W. (2017), "Site response analysis of vertical ground motion in consideration of soil nonlinearity", *Soil Dyn. Earthq. Eng.*, **102**, 124-136. https://doi.org/10.1016/j.soildyn.2017.08.024.

Vamvatsikos, D. and Cornell, C.A. (2002), "Incremental dynamic analysis", *Earthq. Eng. Struct. Dyn.*, **31**(3), 491-514. https://doi.org/10.1002/eqe.141.

XTRACT v3.0.7. (2006), Cross-sectional structural analysis of components, Imbsen Software Systems, Sacramento, California, U.S.A.

Yniesta, S., Brandenberg, S.J. and Shafiee, A. (2017), "ARCS: A one dimensional nonlinear soil model for ground response analysis", *Soil Dyn. Earthq. Eng.*, **102**, 75-85. https://doi.org/10.1016/j.soildyn.2017.08.015.

Zhu, C. and Thambiratnam, D. (2016), "Interaction of geometry and mechanical property of trapezoidal sedimentary basins with incident SH waves", *B. Earthq. Eng.*, **14**(11), 2977-3002. https://doi.org/10.1007/s10518-016-9938-z.

Zhu, C., Chavez-Garcia, F.J., Thambiratnam, D. and Gallage, C. (2018), "Quantifying the edge-induced seismic aggravation in shallow basins relative to the 1D SH modelling", *Soil Dyn. Earthq. Eng.*, **115**, 402-412. https://doi.org/10.1016/j.soildyn.2018.08.025.

GC